



HAL
open science

Glycerol and natural sugar-derived complex modulate differentially stratum corneum water-binding properties and structural parameters in an in vitro Raman-desorption model

Joachim Fluhr, Ali Tfayli, Razvigor Darlenski, Maxim Darvin, Nicolas Joly-Tonetti, Nadège Lachmann

► **To cite this version:**

Joachim Fluhr, Ali Tfayli, Razvigor Darlenski, Maxim Darvin, Nicolas Joly-Tonetti, et al.. Glycerol and natural sugar-derived complex modulate differentially stratum corneum water-binding properties and structural parameters in an in vitro Raman-desorption model. *Journal of Biophotonics*, 2022, 16 (1), 10.1002/jbio.202200201 . hal-04343417

HAL Id: hal-04343417

<https://hal.science/hal-04343417>

Submitted on 4 Apr 2024

HAL is a multi-disciplinary open access archive for the deposit and dissemination of scientific research documents, whether they are published or not. The documents may come from teaching and research institutions in France or abroad, or from public or private research centers.

L'archive ouverte pluridisciplinaire **HAL**, est destinée au dépôt et à la diffusion de documents scientifiques de niveau recherche, publiés ou non, émanant des établissements d'enseignement et de recherche français ou étrangers, des laboratoires publics ou privés.

RESEARCH ARTICLE

Glycerol and natural sugar-derived complex modulate differentially stratum corneum water-binding properties and structural parameters in an in vitro Raman-desorption model

Joachim W. Fluhr^{1,2}  | Ali Tfayli³  | Razvigor Darlenski^{4,5}  |
Maxim E. Darvin^{6,7,8}  | Nicolas Joly-Tonetti⁹ | Nadège Lachmann⁹

¹Charité—Universitätsmedizin Berlin, Institute of Allergology, Berlin, Germany

²Allergology and Immunology, Fraunhofer Institute for Translational Medicine and Pharmacology ITMP, Berlin, Germany

³Lipides: Systèmes Analytiques et Biologiques, Lip(Sys)2, Faculty of Pharmacy, Paris-Saclay University, Orsay, France

⁴Department of Dermatology and Venereology, Acibadem City Clinic Tokuda Hospital—Sofia, Sofia, Bulgaria

⁵Department of Dermatology and Venereology, Medical Faculty, Trakia University-Stara Zagora, Stara Zagora, Bulgaria

⁶Department of Dermatology, Venereology and Allergology, Center of Experimental and Applied Cutaneous Physiology (CCP), Charité—Universitätsmedizin Berlin, Berlin, Germany

⁷Freie Universität Berlin, Berlin, Germany

⁸Humboldt-Universität zu Berlin, Berlin, Germany

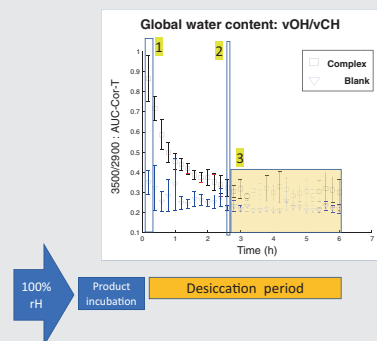
⁹Scientific and Claims Development, Galderma SA, Lausanne, Switzerland

Correspondence

Joachim W. Fluhr, Charité—Universitätsmedizin Berlin, Institute of Allergology, Campus Benjamin Franklin, Hindenburgdamm 30, Haus II, 12203 Berlin, Germany.
Email: joachim.fluhr@charite.de

Abstract

The epidermal protective functions are closely associated with skin hydration homeostasis. The understanding of different states of water binding is a rising concept in assessing topically applied formulations and their interaction within the stratum corneum (SC). In addition to global water content, primary bound water, partially bound water, and unbound water and barrier-related lipid lateral packing and protein secondary structure can be measured by Raman spectroscopy. This study aimed to establish an in vitro SC model to evaluate differences in the efficacy of a natural sugar-derived complex in combination with glycerol and a botanical extract in modulating SC water binding and structural proteins and barrier lipids. These compounds were selected due to their water-binding and soothing properties. The SC water profiles were assessed at the surface and in 8 μm SC depth. After a 12-hour hyperhydration and subsequent product incubation the measurements were performed during a 6 hours desiccation phase. The maximal water caption and the time until reaching a steady state are measured as well as water retention and resistance against water loss. Global water content, partially bound, and unbound water, as well as lipid and protein structures were assessed with confocal Raman microspectroscopy. Both the natural sugar-derived mixture and more pronounced, the same mixture with additional glycerol increased all three water-binding parameters at the surface and in 8 μm SC depth at the beginning and during the desiccation phase. Further addition of botanical extract did not result in an additional increase of the water-binding. All three formulations showed an increase in the lipid lateral



This is an open access article under the terms of the [Creative Commons Attribution](https://creativecommons.org/licenses/by/4.0/) License, which permits use, distribution and reproduction in any medium, provided the original work is properly cited.

© 2022 The Authors. *Journal of Biophotonics* published by Wiley-VCH GmbH.

Funding information

Galderma, Grant/Award Number:
Research funded by Galderma

packing values prevented the protein alteration as measured by β -sheets signal compared to blank. The present model is suited for screening studies comparing the specific effects of different compounds on hydration states. The natural sugar-derived mixture Aquaxyl showed evidence for an improvement of all SC hydration states, lipid and protein structure which was further enhanced by the addition of glycerol 5%. This improvement was evidenced at the surface and within the SC for all hydration-related parameters, and the lipid as well the protein structures. The addition of botanical extract phytoessence blue daisy did not show further improvement.

KEYWORDS

dry skin, in vitro model, lipid lateral packing, partially bound water, Raman spectroscopy, β -sheet signal, stratum corneum hydration, unbound water, water binding capacity, xerosis

1 | INTRODUCTION

The multiple protective functions of the epidermal barrier are widely dependent on the skin hydration homeostasis [1]. Stratum corneum (SC), the outermost skin layer mainly responsible for the barrier function, accomplishes the adaptation of the skin from *utero* to the relatively dry terrestrial surrounding environment [2]. The regulatory mechanisms that SC exerts for maintaining optimal hydration include barrier function, water binding, and SC water diffusion [3]. The water handling properties are mainly dependent on the highly hygroscopic natural moisturizing factor (NMF) complex (mainly filaggrin-derived), and the SC intercellular lipids (ICL) organized in lamellas by lateral packing and the optimal ratio between orthorhombic and hexagonal structures [4, 5]. The organization of ICL lamellar structures is an important regulator of the transepidermal water loss (TEWL) [6], thus forming the major diffusion water pathway in the SC [7]. Higher water evaporation from the skin surface (higher TEWL value) is indicative of permeability barrier disturbance as in atopic dermatitis, ichthyosis vulgaris, and xerosis cutis [8, 9]. Different types of water binding states in the SC can be called primary bound, partially bound and unbound water mobility states [3, 10]. The content of bound water is related to the lipid profile in SC [11]. The most tightly bound water has its highest concentration near the skin surface and is not responsible for the TEWL [10]. The hydrogen bonding state of water increases up to the depth of 30% of the SC thickness, which correlates well with the lateral packing order of ICL and the NMF maxima, with the dominance of the latter concerning the water bonding [10]. A comparison of porcine and human SC showed stronger water binding in the upper human SC [12].

In an additional series of Raman-spectroscopy-based human in vivo studies, a distinction between water-binding mobility states was described for the SC depth-dependently [10, 13]. According to the strength of its hydrogen bonds with the surrounding molecules, SC water could be in four binding states: single donor-double acceptor (DAA, tightly bound water), double donor-double acceptor (DDAA, strongly bound water), single donor-single acceptor (DA, weakly bound water) and free water, which can be measured by the Gaussian function-based deconvolution of the Raman OH band (3100 to 3700 cm^{-1}) [10]. Dry skin is characterized by a decreased water content of skin surface and SC. To determine water concentration in the SC the normalization on the keratin CH_3 band (2910 to 2965 cm^{-1}) is usually performed [14], which has a number of limitations in case of the treated skin [12]. To minimize these limitations a normalization to the amid I band at 1650 cm^{-1} was proposed [15]. This adaptation is currently under discussion [16, 17]. Another normalization-free algorithm is recently introduced and based on the application of tailored multivariate curve resolution-alternating least squares (tMCR-ALS) method [18, 19].

Changes in ambient air relative humidity (RH) exert relevant effects on the epidermal barrier structure and functions. Lower RH results in a decrease in the water amounts in the SC [20], increased dry weight of the SC and epidermal thickness [21], an increase or decrease in the lamellar bodies number [22, 23], and modification of keratin chains [20]. Upon dehydration, epidermal DNA synthesis and the number of keratohyalin granules are enhanced [21, 24]. The dynamic changes in TEWL in low RH are accompanied by decreased filaggrin levels, suggesting engagement of the protein breakdown in the restoration of SC hydration [24, 25]. Delayed epidermal barrier restoration is seen with prior exposure to a humid

environment [22]. The decreased tensile properties of the skin in a dry environment are clinically observed as enhanced desquamation and xerosis [20].

Water profile and handling properties, together with SC lipid and keratin conformational changes have been studied in an *ex vivo* drying skin model [20] and in human SC *in vivo* [26]. Emollient molecules showed enhanced water retention capacity of the SC and lipid conformation [27]. Humectants, defined as substances capable of retaining or preserving moisture, are widely used in the treatment and prevention of dry skin. Glycerol at 3% to 5%, an endogenously synthesized highly hygroscopic trihydroxy alcohol, increases skin hydration, improves skin barrier function by preventing phase transition of SC lipids, promotes skin mechanical properties, protects against irritating stimuli, enhances desmosomal degradation, and accelerates wound healing processes [28]. Natural plant sugars derivatives, namely xylitylglucoside, anhydroxylitol, and xylitol boost skin hydration, and reinforce skin barrier [29]. Iridoide glycosides containing blue daisy botanical extract suppresses skin inflammation by inhibiting the secretion of interleukin 8 and prostaglandin E2 and soothe the skin [30–32]. While glycerol and xylitol can be associated to improve skin hydration status [33], associating both with a prostaglandin E2-targeting material could benefit to dry, dehydrated sensitive skin. The present study contributes to the understanding of a classic moisture enhancing agent such as glycerol and its effect on different states of water binding and SC structure.

This study aimed to differentiate several hydrating compounds regarding their influence on global water content and on water-binding states (particularly partially bound and unbound water) at the surface and within the SC in a dynamic hydration-dehydration model. In addition, we aimed to evaluate the efficacy of glycerol, a natural sugar-derived complex and plant extract in enhancing SC water-binding properties and stabilizing structural lipid and protein components in the SC.

We propose five hypotheses about water binding states in the SC, which maintain the entire SC hydration as follows:

1. A basic mixture of polyalcohols and the sugar alcohols (Aquaxyl 2%) (mixture 1.1) can increase SC water content both at the surface and deeper parts of the SC for all water mobility states.
2. The addition of glycerol 5% to the basic mixture (mixture 1.2) increases the positive effect of mixture 1.1 on the SC water content both at the surface and deeper parts of the SC for all three water mobility states.
3. The addition of a botanical extract phytoessence blue daisy to mixture 1.2 (complex 1) increases the positive effect of mixture 1.2 on the SC water content both at the surface and deeper parts of the SC for all water mobility states.
4. All three formulations have a positive effect (protection against the lipid-disorganizing effect of hyperhydration) on the lipid lateral packing in the SC as a marker for barrier-related lipid structure.
5. All three formulations have a positive effect (protection against the protein-structure impairment in the hyperhydration model) on the relative amount of secondary β -sheet keratin structure as a prerequisite for enhanced water binding.

2 | MATERIAL AND METHODS

2.1 | SC overhydration—desiccation—model

Two isolated human SC samples were used from two different donors. The study was approved by the local ethics committee of the analyzing institute (Université Paris-Saclay). The methods were applied as previously described [3]. Briefly, a droplet of distilled water was applied on a CaF₂ slide. Isolated SC samples were spread on the slide and dried with absorbent paper. Samples were dried at room temperature 21°C and room RH of 40% for 3 hours. Subsequently, the SC samples were incubated in a chamber at >90% RH for 12 hours (overnight). 50 μ l of the different formulations or water were incubated again at >90% RH for 2 additional hours. During the desiccation phase, the RH was set down to 4% to 7% in the climate chamber. The desiccation process was monitored over 6 hours.

Confocal Raman microspectroscopy monitored water content, lipid lateral packing, and protein secondary structure in terms of the relative amount of β -sheet keratin. The SC water profiles were assessed near the surface and at the depth of 8 μ m to show the effect of a dehydrating external environment at the surface and in the deeper SC depth.

2.2 | Confocal Raman microspectroscopy

Raman spectral collection was performed using a Lab-RAM HR evolution Raman microspectrometer (Horiba Scientific, Lille, France). A 633 nm laser (Toptica Photonics, Munich, Germany) was used as an excitation source. The laser was focused on the sample with a long focal microscope objective PL Fluotar L 100X/NA 0.75 WD 4.7

(Leica, Mannheim, Germany). The confocal hole was set at 200 μm for all measurements.

Spectral acquisitions were performed using Labspec 6 software (Horiba Scientific, Lille, France). Raman measurements were performed in the 400 to 3800 cm^{-1} spectral range. For each spectral acquisition two times 5 seconds collection was used. The spectral collection was performed from $-10 \mu\text{m}$ (out of the SC) down to 40 μm (below the SC surface) with a 2- μm increment. The 50 μm in the depth movement for the depth profile was chosen to take into account the modifications in the SC thickness along the drying process. The SC surface and the interface between SC and the CaF_2 slide positions were corrected as detailed by Galliano et al [34].

The collection was then repeated 40 times for a total of 6 hours. All spectra were smoothed using the Savitzky-Golay algorithm on 11 points and baseline corrected using an automatic polynomial function.

The drying process of the SC samples was monitored using the following parameters: the content of global water in the SC was evaluated using the area under the curve (AUC) of the OH stretching νOH band (3100 to 3700 cm^{-1}) [3, 20]. Water binding state was assessed from the subbands of the νOH band: the spectral region 3250 to 3450 cm^{-1} is associated with partially bound water while the vibrations in the 3450 to 3600 cm^{-1} region are due to unbound water [3, 20]. Global water content was analyzed using the AUC of the OH stretching in the region 3100 to 3700 cm^{-1} . The ratio between the AUC of OH stretching and CH stretching ($\approx 2900 \text{ cm}^{-1}$) bands was calculated. Partially bound water was analyzed in the spectral region 3250 to 3450 cm^{-1} . Unbound water (free water) was analyzed using the vibration in the spectral region 3420 to 3600 cm^{-1} .

Lipids lateral packing was assessed by following the $\nu_{\text{asym}}\text{CH}_2$ (2880 cm^{-1})/ $\nu_{\text{sym}}\text{CH}_2$ (2850 cm^{-1}) ratio. High values are associated with higher conformational order and a compact organization of lipids. $\nu_{\text{asym}}\text{CH}_2$ (2882 cm^{-1})/ $\nu_{\text{sym}}\text{CH}_2$ (2852 cm^{-1}) asymmetric to symmetric CH_2 stretching vibration intensity ratio is used as a parameter of the lateral packing order of the lipids. Higher values are associated with an increase in lateral lipid packing and a more compact organization indicating a positive effect on the epidermal barrier.

The Amide I band is directly related to the secondary structure of proteins. It can be composed into several subbands associated with different forms of secondary structure; that is, α -helix, β -sheet, and random coil structures. It has been previously shown that at high RH% affects the secondary structure with a decrease of the relative amount of β -sheet keratin [3, 20].

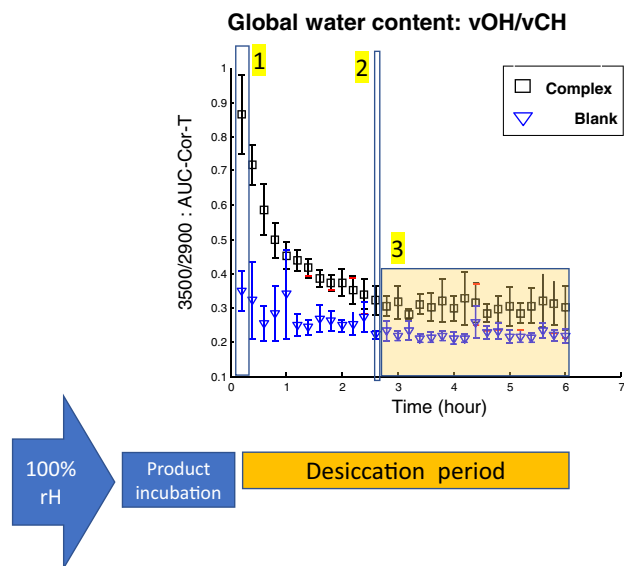


FIGURE 1 Schematic representation of the study design. Global water content ($\nu\text{OH}/\nu\text{CH}$) with an initial exposure to 100% relative humidity (RH) (blue arrow) followed by product incubation (blue bar). At the end of the pretreatment period, the desiccation process started (orange bar). The desiccation phase starts at point 1 going into the desiccation phase until reaching a steady state at point 2. Point 1 represents the water caption at 100% RH. Point 2 is delayed in reaching the steady-state if water-binding components are applied to the SC indicating water retention and increased resistance against water loss. The plateau 3 represents the amount of water holding capacity of the SC over several hours

Both lipid lateral packing and protein structure were assessed in the depth of 0 to 4 μm .

The different phases of the desiccation process are explained in Figure 1 in an example of desiccation or “drying” profiles for global water content are plotted for complex 1 against untreated SC (green rings). The profiles are obtained at the surface of SC over 6 hours. The prehydration (12 hours blue flesh overnight) and incubation with the different formulations for 2 hour (blue bar) are performed before the 6 hours desiccation time (orange block). Only the desiccation period was monitored by confocal Raman microspectroscopy. The box at yellow flag number 1 represents the initial water caption at a fully hydrated and pretreated state obtained at the beginning of the drying process. Yellow flag number 2 shows the delay (time) from the starting point 1 to reach the plateau of desiccation representing the water retention capacity (resistance against water loss by desiccation). Water holding capacity is represented by the period starting at the yellow flag number 3 throughout the remaining time of desiccation (yellow translucent box). This period represents the water that can be kept in the SC after reaching the plateau.

The validation of this method in the process of ingredient screening in a SC model was performed as following.

2.3 | Ingredient selection

Polyalcohols and sugar alcohols are known humectants, glycerol and xylitol being effective together for skin hydration [33]. To test the functionality of the different ingredients in an aqueous solution without losing the advantage of additive moisturizing and soothing effects of several combined molecules the combinations of the ingredients were tested *ex vivo* on the isolated and prehydrated SC.

2.3.1 | Mixture 1.1

Aquaxyl formulation was selected as a mixture with the ability to form hydrocolloids due to its high water-binding capacity [35]. Aquaxyl 2% (in distilled water) is a trademark-protected mixture of polyalcohols and the sugar alcohols xylitylglucoside, anhydroxylitol, and xylitol (SEPPIC S.A., 22 Terrasse Bellini, 92 806 Puteaux, France).

2.3.2 | Mixture 1.2

Mixture 1.2 is the same as mixture 1.1 with the addition of glycerol 5% (Vantage, 1751 Lake Cook Road, Suite 550, Deerfield, IL 60 015, USA). Glycerol at low concentration is known for its improvement of SC hydration, skin barrier function and skin mechanical properties, inhibition of the SC lipid phase transition, and protection against irritating stimuli [28, 36].

2.3.3 | Complex 1

Complex 1 is the same as mixture 1.2 with the addition of phytoessence blue daisy 0.15% (*Globularia alypum* leaf botanical extract) (Crodarom, ZA «Les Plaines», 48 230 Chanac, France). The rationale for adding phytoessence blue daisy was its ability of skin-soothing and anti-inflammatory properties due to the high content of glycosyl-iridoids, lignan and cinnamyl acetates (liriodendrin, globularin, globularinin, and syringing) [37, 38]. These compounds have been associated as there is emerging evidence about additive, complementary, and synergistic effects [33, 39, 40].

2.4 | Statistical analysis

Kruskal Wallis (KW) was performed between the groups. It is a nonparametric (distribution-free) test used to compare independent groups of sampled data. Unlike the parametric independent group analysis of variance (ANOVA) (one-way ANOVA), this nonparametric test makes no assumptions about the distribution of the data (eg, normality). It is used to compare samples from two or more groups. In our work KW was used pairwise and the obtained *P*-values were color coded ($P < .01$ [dark green], $P < .05$ [light green], $P < .1$ [yellow] and $P > .1$ [black]). To validate the results, a pairwise comparison based on Bonferroni test was performed using multicompare function in Matlab. In Figures 2 to 5 each line of the color coded results indicate the two groups between which it was performed, that is: Mix 1.1 vs Mix 1.2, Cp 1 vs Mix 1.2, Cp 1 vs Mix 1.1, Mix 1.2 vs Blank, Mix 1.1 vs Blank, Cp1 vs Blank. each represents the drying time. For example, if the reader look to the square (pixel) at first column and the last line it represent the KW *P*-value calculated between CP1 and the blank at the beginning of the drying process.

The overall effects were assessed with a semi-quantitative score using a three grade scale (+mild improvement, ++moderate improvement, +++marked improvement). This simplifying score was used to give an overall summary of the complex results of different ingredient combinations in relation to the different assessed SC depth. No formal validation was performed for this semi-quantitative assessment.

3 | RESULTS

3.1 | Validity of the model

Figure 1 illustrates the model with different hydration states during the product incubation and the desiccation period over the following 6 hours. The desiccation phase starts at point 1 going into the desiccation phase until reaching a steady state at point 2. Point 1 represents the water caption at 100% RH. Point 2 is delayed in reaching the steady-state if water-binding components are applied to the SC indicating water retention and increased resistance against water loss. The plateau 3 represents the amount of water holding capacity of the SC over several hours. With the present study, we were able to differentiate different water binding states in the SC.

Global water content: vOH/vCH

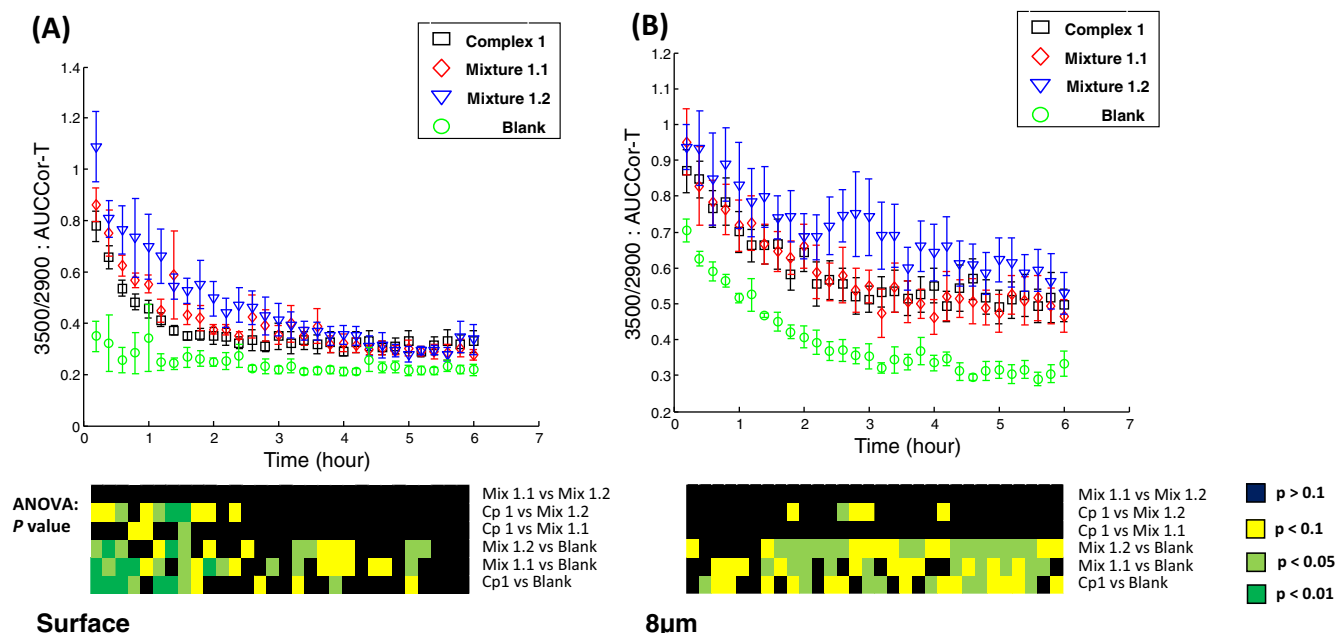


FIGURE 2 Global water (ratio of AUC of the OH stretching band (3100 to 3700 cm^{-1}) to the AUC of the CH_3 stretching band (2800 to 3000 cm^{-1})) over the 6 hours of dehydration process at the surface and in $8\text{ }\mu\text{m}$ SC depth. Panel A: Global water at the SC surface. Panel B: Global water at $8\text{ }\mu\text{m}$ SC depth. The statistical analysis (KW followed by pairwise comparison) is depicted in a color-coded map (black = n.s., yellow $P < .1$ [trend], light green $P < .05$, dark green $P < .01$). Most of the differences are seen in the first 2 hours for the surface measurements and over the entire 6 hours in $8\text{ }\mu\text{m}$ depth

3.2 | Global water content

The water content (Figure 2) was evaluated at the SC surface (Figure 2A) and $8\text{ }\mu\text{m}$ SC depth (Figure 2B). The changes compared to untreated SC (blank SC without compound application [green rings]) for all water states are summarized in Table 1.

At the SC surface (Figure 2A) the plateau was already reached after 1 hour in untreated SC. Adding Aquaxyl 2% (mixture 1.1) to the SC increased the time to reach the plateau to 2 hours (red diamonds) and further increased to 3.5 hours with additional glycerol 5% (mixture 1.2) (blue triangles). Both mixture 1.1 and 1.2 increase the water content at the beginning of the desiccation phase (water caption at 100% RH), during desiccation, and over the steady-state with an advantage of mixture 1.1 over mixture 1.2 specifically, in the early phase of desiccation. The addition of phytoessence blue daisy to mixture 1.1 complex 1 did not increase water at the surface. However, the water binding capacity in the later desiccation phase after 3.5 hours was comparable to that of both mixtures and higher than the control (blank).

When looking into the SC at a depth of $8\text{ }\mu\text{m}$ (Figure 2B) all three formulations had a comparable increase of the initial water content with comparable

water caption values compared to blank. The highest water retention and resistance against water loss was seen with Aquaxyl plus glycerol (mixture 1.2) reaching the plateau only after approx. 4.5 hours while Aquaxyl alone (mixture 1.1) and Complex 1 showed similar behavior reaching their respective plateaus after approx. 3 hours. The plateaus of all three formulations were higher than untreated SC indicating a significantly increased water holding capacity over the entire desiccation process. The Aquaxyl plus glycerol (mixture 1.2) showed the highest water content for resistance against water loss and water holding capacity over the 6 hours test period.

3.3 | Structural water-binding: partially bound water

The partially bound water (Figure 3) was tested at the SC surface (Figure 3A) and $8\text{ }\mu\text{m}$ SC depth (Figure 3B). At the SC surface (Figure 3A) the plateau in untreated SC was reached after 1 hour. Treating the SC with mixture 1.1 increased the time to reach the plateau to 2.5 hours (red diamonds) and further increased to 3.5 hours by adding glycerol 5% (mixture 1.2) (blue triangles) representing

Partially bound water profiles (3245-3420 cm⁻¹ are associated with partially bound water)

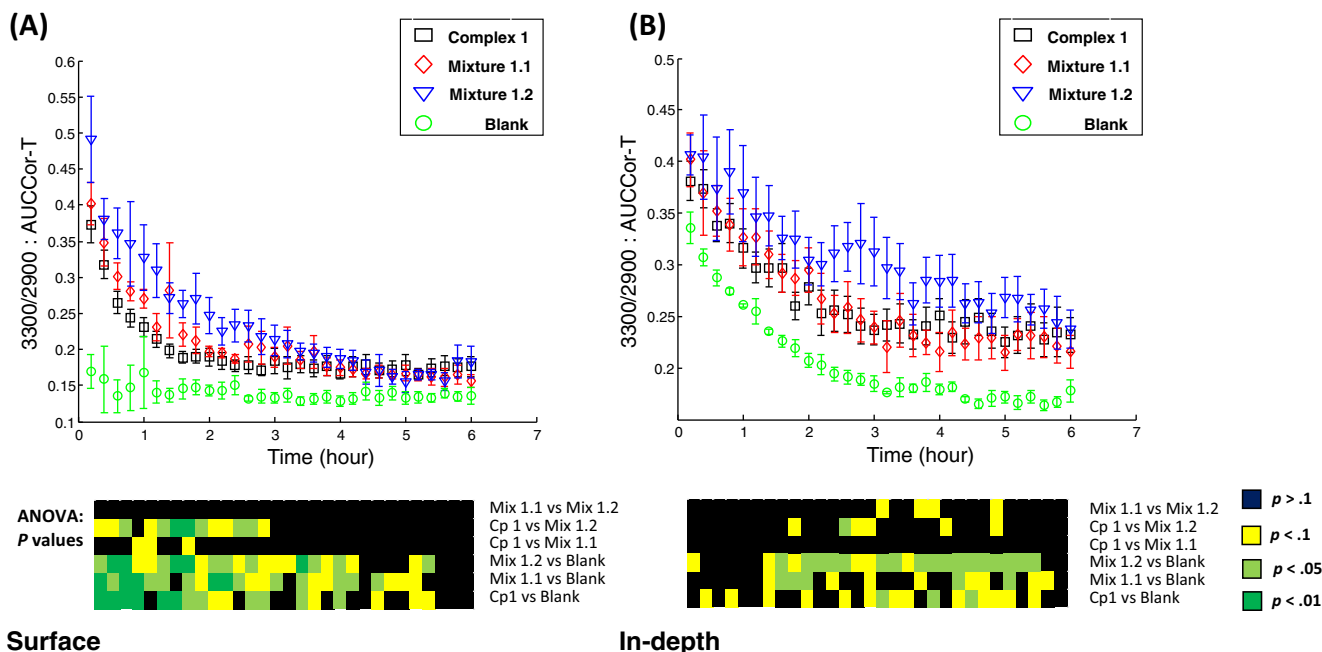


FIGURE 3 Partially bound water content over the 6 hours desiccation process at the surface and at 8 μm SC depth. Panel A: Partially bound water content at the SC surface. Panel B: Partially bound water content at 8 μm SC depth. The statistical analysis (KW followed by pairwise comparison) is depicted in a color-coded map (black = n.s., yellow $P < .1$ [trend], light green $P < .05$, dark green $P < .01$). Differences are seen in the for the surface measurements and in 8 μm depth over the entire 6 hours

Unbound water profiles (3420-3600 cm⁻¹ are associated with unbound)

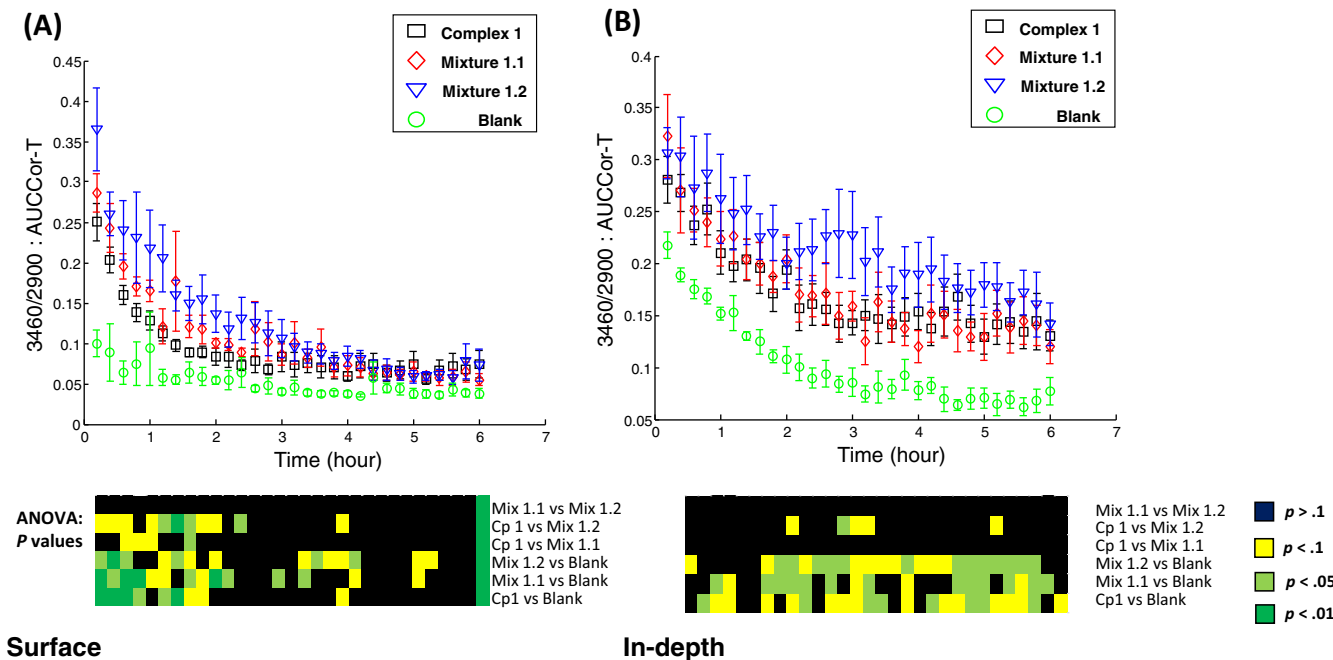
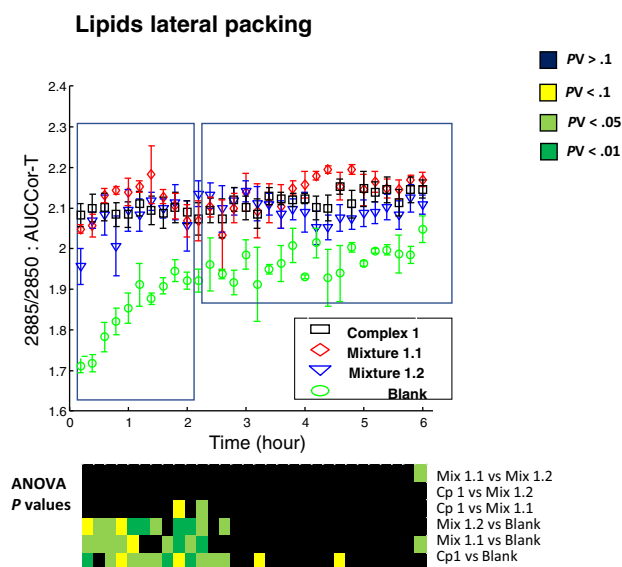


FIGURE 4 Unbound water content over the 6 hours desiccation process at the surface and in 8 μm SC depth. Panel A: Unbound water content at the SC surface. Panel B: Unbound water content at 8 μm SC depth. The statistical analysis (KW followed by pairwise comparison) is depicted in a color-coded map (black = n.s., yellow $P < .1$ [trend], light green $P < .05$, dark green $P < .01$). Most of the differences are seen in the first 2 hours for the surface measurements and over the entire 6 hours in 8 μm depth

an increased resistance against water loss. Both mixtures also increased the total amount of partially bound water at the beginning of the desiccation phase (water caption at 100% RH), during desiccation, and over the steady-state with an advantage of mixture 1.2 over mixture 1.1. With complex 1 the increase in partially bound water regarding the water retention rate was slightly less pronounced compared to mixture 1.2, but comparable to mixture 1.1. However, the water-binding capacity after

3.5 hours was comparable for both mixtures and complex 1 and higher than in untreated SC.

Analyzing at the 8 μm SC depth (Figure 3B) all three formulations had a comparable significant increase of the initial content of partially bound water compared to blank. The highest water retention rate and resistance against water loss were seen in mixture 1.2-treated SC reaching the plateau after approx. 4.5 hours while Aquaxyl alone (mixture 1.1) and Complex 1 showed similar behavior reaching their respective plateaus already after approx. 3 hours. The plateaus of all three formulations were higher than untreated SC indicating a relevant increased partially bound water holding capacity and resistance against water loss. Mixture 1.1 showed the highest partially bound water values for resistance against water loss and water holding capacity over the entire test period.



Asymmetric to symmetric CH_2 stretching ratio

FIGURE 5 Lateral packing order of SC lipids in the depth of 0 to 4 μm . The statistical analysis (KW followed by pairwise comparison) is depicted in a color-coded map (black = n.s., yellow $P < .1$ [trend], light green $P < .05$, dark green $P < .01$). Most of the differences are seen in the first 2 hours

3.4 | Structural water-binding: unbound water

The unbound water (Figure 4) was tested at the SC surface (Figure 4A) and 8 μm SC depth (Figure 4B). At the SC surface (Figure 4A) the plateau for unbound water was reached after 1 hour in untreated SC (green ring). Treating the SC with Aquaxyl 2% (mixture 1.1) increased the time to reach the plateau to 2.5 hours (red diamonds) and further increased to 4.0 hours by adding glycerol 5% (blue triangles) representing an increased resistance against water loss of unbound water. Both mixtures also increased the total amount of unbound water at the beginning of the desiccation phase. During the desiccation phase mixture 1.2 showed a slight advantage over mixture 1.1. With complex 1 the increase in unbound

TABLE 1 Summarizing the effects of the three formulations in compared to untreated stratum corneum (blank) at the surface and 8 μm depth measurement

	Global water	Partially bound water	Unbound water	
Mixture 1.1				
Surface	+	+	++	Early phase (until 3 hours)
8 μm	++	++	++	3 to 6 hours (plateau)
Mixture 1.2				
Surface	++	+	++	Early phase (until 3 hours)
8 μm	+++	+++	+++	3 to 6 hours (plateau)
Complex 1				
Surface	+	+	++	Early phase (until 3 hours)
8 μm	++	++	++	3 to 6 hours (plateau)

Note: Global water content, partially bound water and unbound water: + mild improvement, ++ moderate improvement, +++ marked improvement compared to blank.

water content was slightly less pronounced compared to both mixtures. However, the water-binding capacity after 3.5 hours was comparable to Aquaxyl and significantly higher than blank.

Analyzing the unbound water at the SC depth of 8 μm (Figure 4B) complex 1 and both mixtures had a comparable increase of the initial content of unbound water compared to blank. The highest water retention and resistance against water loss was seen in mixture 1.2 with reaching the plateau after approx. 4.5 hours while mixture 1.1 and complex 1 showed similar behavior reaching their respective plateaus already after approx. 3 hours. The plateaus of all three formulations were higher than untreated SC indicating a relevant increased water holding capacity of unbound water and resistance against water loss. Mixture 1.2 showed the highest unbound water values for resistance against water loss and water holding capacity.

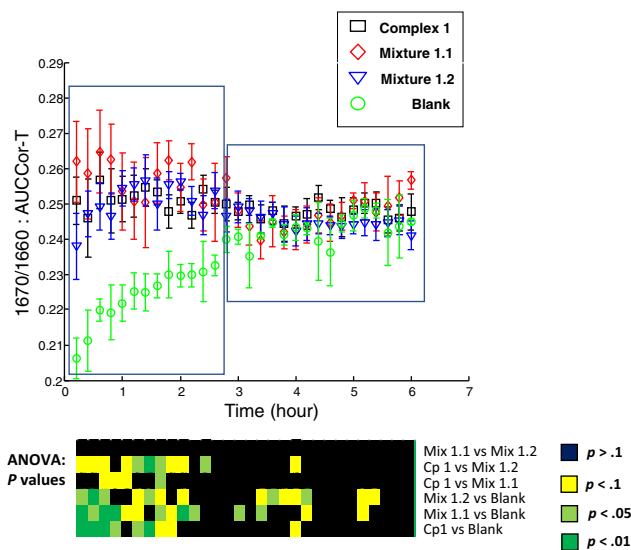
3.5 | Lateral packing order of SC lipids (2882 cm^{-1} /2852 cm^{-1} intensity ratio)

The dynamic of lateral packing order of lipids is depicted in Figure 5. Hyperhydration (exposure to 100% RH) lead to a decrease in lipid lateral packing in untreated SC. It is of notice that the lipid compactness is decreased by the hyperhydration. A minimal initial decreased lipid lateral packing was observed with mixture 1.2 that recovered within 1 hour. All three formulations showed an increase in the lateral packing values compared to blank. This is indicative of the prevention of a decrease of lipid lateral packing by all formulations in the hyperhydration-desiccation model.

3.6 | Protein secondary structure: Relative amount of β -sheet keratin (1665 to 1680/[1600 to 1700] amid I band)

The amid I band is related to the secondary structure of proteins. It can be divided into sub-bands associated with different forms of secondary structures; for example, α -helix fibers, β -sheet ribbons, and random coil structures. Figure 6 shows that the overnight exposure of the SC to 100% RH induced a decrease of the β -sheet keratin, which recovered during the desiccation process within 3 hours (blank; green circles). All three formulations prevented the alteration of the β -sheet keratin. In the initial phase of the desiccation process, Mixture 1.2 showed a slight impairment of the β -sheet values which recovered within 1 hour. All three formulations-treated SC showed higher values in the protein secondary structure

Protein secondary structure



Relative amount of β sheets

FIGURE 6 Proteins secondary structure in the depth of 0 to 4 μm . The statistical analysis (KW followed by pairwise comparison) is depicted in a color-coded map (black = n.s., yellow $P < .1$ [trend], light green $P < .05$, dark green $P < .01$). Most of the differences are seen in the first 2 hours for the surface measurements and over the entire 6 hours in 8 μm depth

compared to blank. This is indicative of the prevention of a negative impact of the protein structure by all formulations in the hyperhydration-desiccation model.

4 | DISCUSSION

We aimed to prove the validity of an in vitro SC model to study the different hydration states as well as barrier-related parameters in terms of lipid lateral packing and the protein secondary structure using confocal Raman microspectroscopy. Furthermore, the Raman spectroscopy-based model served to dissect the efficacy of different mixtures of topical ingredients.

The interactions between the SC and mixture of active ingredients are highly complex. This investigation should request another technique than Raman spectroscopy and is not the purpose of this article. We intended to demonstrate any additive/superior efficacy of combining different active ingredients for topical preparations. Peer-reviewed and published studies were conducted in the past to understand the interaction of single materials with the SC using Raman [41]. An initial study to investigate the combination of ingredients has already been published, with a positive impact in both dermatology and Raman literature [20].

Our hypothesis could be answered as follows (summarized in Table 1): (a) the basic mixture of polyalcohols and the sugar alcohols (Aquaxyl 2%) (mixture 1.1) was able to increase SC global water content both at the surface and at 8 μm SC depth, in particular for partially bound and unbound water mobility states. (b) The addition of glycerol 5% to the basic mixture (mixture 1.2) increased the positive effect of mixture 1.1 on the SC water content both at the surface and at 8 μm SC depth for different water mobility states. (c) The addition of the botanical extract phytoessence blue daisy to mixture 1.2 (complex 1) did not further increase the positive effects of mixture 1.2 on the SC water content both at the surface and deeper parts of the SC for different water mobility states. The hydrating effect of complex 1 was equal to that of mixture 1.1, thus hypothesis iii must be rejected. (d) All three formulations showed a positive effect (protection against the hyper-hydration) on the lipid lateral packing in the SC as a marker for barrier-related lipid structure. (e) All three formulations protected the number of β -sheet keratin as a marker for barrier-related protein structure.

The model was able to show that all three mixtures were able to induce an increase in SC hydration with the best highest water-binding capacity for mixture 1.2 with no further increase of water binding by the addition of phytoessence blue daisy. Here, we showed the present model is a valid screening model for dynamic hydration changes and can differentiate between the proposed different water mobility states. The differentiation is important in the prevention and correction of SC desiccation as seen in the clinical context of hand dermatitis, for example, during washing procedures [42]. The desiccation curve is comparable to the slower/late desiccation in over-hydrated clinical conditions [43, 44].

The Raman-spectroscopy-based model could differentiate the effect of specific active ingredients which leads to the design of targeted formulations regarding protective/regenerative effects on the different states of water and the dynamics of hydration. Especially the sequential addition of new ingredients can be studied in detail, for example, the immediate effect of hydration on water binding capacity. The results might be further verified in the in vivo sorption-desorption test [45, 46]. Future research will address the following points: screening the effect of different formulations on the SC, comparing SC from different anatomical localizations regarding their water binding properties and comparing SC from diseased donors (eg, atopic dermatitis, sensitive skin).

We could also show that this is a semi-qualitative model for the quality of the lipid organization in a hyper-hydration—desiccation model. The different SC hydration states were previously studied in relation to occlusion and a corresponding SC swelling [4]. The authors

showed a shift of water-binding from a more strongly bound state to a weak hydrogen bonding state under occlusion. This effect was most pronounced in the upper SC. In a murine model occlusion induced a disturbance in lipid lamellar membrane structure and the lamellar bodies [47].

Initially, over-hydration induced a decrease in the quality of lipid and protein secondary structure, which could be prevented by all three mixtures. This protection was seen in the early desiccation phase (0 to 2 hours after hyper-hydration and product application) and the later phase (2 to 6 hours) with no relevant changes over the entire time.

In conclusion, the present model is suited for screening studies especially comparing the specific effects of different compounds. Aquaxyl showed evidence for an improvement of all SC hydration states, lipid, and protein structure which was further enhanced by the addition of glycerol 5%. The addition of botanical extract phytoessence blue daisy did not show further improvement. The three mixtures were able to protect the lipid as well the protein structure. The practical application of our results could be the implementation of natural sugar-derived complexes to classical moisturizers as potential topical skin formulations' ingredients. The clinical relevance of the present in vitro data needs to be confirmed by testing in a controlled, double-blinded, prospective in vivo study.

ACKNOWLEDGMENTS

JWF and RD have received consulting fees from Galderma in the past. AT performed the in vitro studies. NJ-T and NL are employees of Galderma. Open Access funding enabled and organized by Projekt DEAL.

FUNDING INFORMATION

This study was sponsored by Galderma, Switzerland.

CONFLICT OF INTEREST

The authors declare no potential conflict of interest.


DATA AVAILABILITY STATEMENT

No additional data available.

ORCID

Joachim W. Fluhr  <https://orcid.org/0000-0003-3610-0698>

Ali Tfayli  <https://orcid.org/0000-0002-9222-2852>

Maxim E. Darvin  <https://orcid.org/0000-0003-1075-1994>

REFERENCES

- [1] C. Choe, J. Schleusener, J. Lademann, M. E. Darvin, *Sci. Rep.* **2017**, *7*, 15900.

- [2] J. W. Fluhr, G. Bellemere, C. Ferrari, C. De Belilovsky, G. Boyer, N. Lachmann, C. P. McGuckin, N. Forraz, R. Darlenski, B. Chadoutaud, P. Msika, C. Baudouin, G. Pellacani, *J. Invest. Dermatol.* **2019**, *139*, 464.
- [3] R. Vyumvuhore, A. Tfayli, H. Duplan, A. Delalleau, M. Manfait, A. Baillet-Guffroy, *Analyst* **2013**, *138*, 4103.
- [4] C. Choe, J. Schleusener, S. Choe, J. Ri, J. Lademann, M. E. Darwin, *Int. J. Cosmet. Sci.* **2020**, *42*, 482.
- [5] V. S. Thakoersing, G. S. Gooris, A. Mulder, M. Rietveld, A. El Ghalbzouri, J. A. Bouwstra, *Tissue Eng. Part C Methods* **2012**, *18*, 1.
- [6] P. M. Elias, G. K. Menon, *Adv. Lipid Res.* **1991**, *24*, 1.
- [7] J. van Smeden, M. Janssens, G. S. Gooris, J. A. Bouwstra, *Biochim. Biophys. Acta* **2014**, *1841*, 295.
- [8] E. M. Rehbindler, K. M. Advocaat Endre, K. C. Lodrup Carlsen, A. Asarnej, K. E. Stensby Bains, T. L. Berents, K. H. Carlsen, H. K. Gudmundsdottir, G. Haugen, G. Hedlin, I. Kreyberg, L. S. Nordhagen, B. Nordlund, C. M. Saunders, L. Sandvik, H. O. Skjerven, C. Soderhall, A. C. Staff, R. Vettukattil, M. R. Vaernesbranden, L. Landro, Study Group, M. H. Carlsen, O. C. L. Carlsen, P. A. Granlund, B. Granum, S. Gotberg, K. Hilde, C. M. Jonassen, U. C. Nygaard, K. Rudi, I. Skrindo, K. Sjoborg, S. G. Tedner, J. Wiik, A. J. Winger, *J. Allergy Clin. Immunol.* **2020**, *8*, 664, e665.
- [9] R. Vyumvuhore, R. Michael-Jubeli, L. Verzeaux, D. Boudier, M. Le Guillou, S. Bordes, D. Libong, A. Tfayli, M. Manfait, B. Closs, *Int. J. Cosmet. Sci.* **2018**, *40*, 549.
- [10] C. Choe, J. Lademann, M. E. Darwin, *Analyst* **2016**, *141*, 6329.
- [11] G. Imokawa, H. Kuno, M. Kawai, *J. Invest. Dermatol.* **1991**, *96*, 845.
- [12] C. Choe, J. Schleusener, J. Lademann, M. E. Darwin, *J. Biophotonics* **2018**, *11*, e201700355.
- [13] C. Choe, J. Schleusener, J. Lademann, M. E. Darwin, *Mech. Ageing Dev.* **2018**, *172*, 6.
- [14] P. J. Caspers, G. W. Lucassen, E. A. Carter, H. A. Bruining, G. J. Puppels, *J. Invest. Dermatol.* **2001**, *116*, 434.
- [15] C. Choe, J. Schleusener, S. Choe, J. Lademann, M. E. Darwin, *J. Biophotonics* **2020**, *13*, e201960106.
- [16] M. E. Darwin, C. Choe, J. Schleusener, S. Choe, J. Lademann, *J. Biophotonics* **2020**, *13*, e2460.
- [17] G. Puppels, P. Caspers, C. Nico, *J. Biophotonics* **2020**, *13*, e202000043.
- [18] C. S. Choe, J. S. Ri, S. H. Choe, P. S. Kim, J. Lademann, J. Schleusener, M. E. Darwin, *J. Raman Spectrosc.* **2022**. <https://doi.org/10.1002/jrs.6349>
- [19] C. Choe, J. Schleusener, J. Ri, S. Choe, P. Kim, J. Lademann, M. E. Darwin, *J. Biophotonics* **2022**, e202200219.
- [20] K. Biniek, A. Tfayli, R. Vyumvuhore, A. Quatela, M. F. Galliano, A. Delalleau, A. Baillet-Guffroy, R. H. Dauskardt, H. Duplan, *Exp. Dermatol.* **2018**, *27*, 901.
- [21] J. Sato, M. Denda, Y. Ashida, J. Koyama, *Arch. Dermatol. Res.* **1998**, *290*, 634.
- [22] M. Denda, J. Sato, Y. Masuda, T. Tsuchiya, J. Koyama, M. Kuramoto, P. M. Elias, K. R. Feingold, *J. Invest. Dermatol.* **1998**, *111*, 858.
- [23] J. Sato, M. Denda, S. Chang, P. M. Elias, K. R. Feingold, *J. Invest. Dermatol.* **2002**, *119*, 900.
- [24] L. Cau, V. Pendaries, E. Lhuillier, P. R. Thompson, G. Serre, H. Takahara, M. C. Méchin, M. Simon, *J. Dermatol. Sci.* **2017**, *86*, 106.
- [25] C. Katagiri, J. Sato, J. Nomura, M. Denda, *J. Dermatol. Sci.* **2003**, *31*, 29.
- [26] M. E. Darwin, J. Schleusener, J. Lademann, C. S. Choe, *Skin Pharmacol. Physiol.* **2022**, *35*, 125.
- [27] C. Choe, J. Schleusener, J. Lademann, M. E. Darwin, *J. Dermatol. Sci.* **2017**, *87*, 183.
- [28] J. W. Fluhr, R. Darlenski, C. Surber, *Br. J. Dermatol.* **2008**, *159*, 23.
- [29] V. R. Leite e Silva, M. A. Schulman, C. Ferelli, J. M. Gimenis, G. W. Ruas, A. R. Baby, M. V. Velasco, M. E. Taqueda, T. M. Kaneko, *J. Cosmetic Dermatol.* **2009**, *8*, 32.
- [30] Q. Ma, Y. Lu, Y. Deng, X. Hu, W. Li, H. Jia, Y. Guo, X. Shi, *BMC Compl. Med. Ther.* **2022**, *22*, 7.
- [31] Y. Li, Y. Yang, X. Kang, X. Li, Y. Wu, J. Xiao, Y. Ye, J. Yang, Y. Yang, H. Liu, *Front. Pharmacol.* **2021**, *12*, 806808.
- [32] E. P. o. Additives, F. Products or Substances used in Animal, V. Bampidis, G. Azimonti, M. L. Bastos, H. Christensen, M. F. Durjava, M. Kouba, M. Lopez-Alonso, S. L. Puente, F. Marcon, B. Mayo, A. Pechova, M. Petkova, F. Ramos, Y. Sanz, R. E. Villa, R. Woutersen, P. Brantom, A. Chesson, J. Westendorf, P. Manini, F. Pizzo, B. Dusemund, *EFSA J.* **2021**, *19*, e06711.
- [33] C. Korponyai, E. Szel, Z. Behany, E. Varga, G. Mohos, A. Dura, S. Dikstein, L. Kemeny, G. Eros, *Acta Derm. Venereol.* **2017**, *97*, 182.
- [34] M. F. Galliano, A. Tfayli, R. H. Dauskardt, B. Payre, C. Carrasco, S. Bessou-Touya, A. Baillet-Guffroy, H. Duplan, *Exp. Dermatol.* **2021**, *30*, 1352.
- [35] K. Salli, H. Anglenius, J. Hirvonen, A. A. Hibberd, I. Ahonen, M. T. Saarinen, K. Tiuhonen, J. Maukonen, A. C. Ouwehand, *Sci. Rep.* **2019**, *9*, 13232.
- [36] M. Breternitz, D. Kowatzki, M. Langenauer, P. Elsner, J. W. Fluhr, *Skin Pharmacol. Physiol.* **2008**, *21*, 39.
- [37] F. Asraoui, A. Kounoun, H. E. Cadi, F. Cacciola, Y. O. E. Majdoub, F. Alibrando, F. Mandolino, P. Dugo, L. Mondello, A. Louajri, *Molecules* **2021**, *26*, 26.
- [38] N. E. Es-Safi, S. Khelifi, A. Kollmann, L. Kerhoas, A. El Abbouyi, P. H. Ducrot, *Chem. Pharm. Bull.(Tokyo)* **2006**, *54*, 85.
- [39] E. Payer, J. Szabo-Papp, L. Ambrus, A. G. Szollosi, M. Andradi, S. Dikstein, L. Kemeny, I. Juhasz, A. Szegedi, T. Biro, A. Olah, *Exp. Dermatol.* **2018**, *27*, 280.
- [40] E. Szel, H. Polyanka, K. Szabo, P. Hartmann, D. Degovics, B. Balazs, I. B. Nemeth, C. Korponyai, E. Csanyi, J. Kaszaki, S. Dikstein, K. Nagy, L. Kemeny, G. Eros, *J. Eur. Acad. Dermatol. Venereol.* **2015**, *29*, 2333.
- [41] R. Vyumvuhore, A. Tfayli, M. Manfait, A. Baillet-Guffroy, *Skin Res. Technol.* **2014**, *20*, 282.
- [42] X. Wang, L. Ye, Q. Lai, S. Wen, Z. Long, X. Qiu, P. M. Elias, B. Yang, M. Q. Man, *Skin Pharmacol. Physiol.* **2020**, *33*, 94.
- [43] H. Tagami, *Int. J. Cosmet. Sci.* **2008**, *30*, 413.
- [44] M. Gloor, B. Wasik, W. Gehring, R. Grieshaber, P. Kleesz, J. W. Fluhr, *Skin Res. Technol.* **2004**, *10*, 1.

- [45] H. Tagami, Y. Kanamaru, K. Inoue, S. Suehisa, F. Inoue, K. Iwatsuki, K. Yoshikuni, M. Yamada, *J. Invest. Dermatol.* **1982**, 78, 425.
- [46] V. Moner, E. Fernandez, A. Del Pozo, G. Rodriguez, M. Cocera, A. de la Maza, O. Lopez, *Contact Dermatitis* **2017**, 77, 25.
- [47] S. Jiang, S. W. Koo, S. H. Lee, *Arch. Dermatol. Res.* **1998**, 290, 145.

How to cite this article: J. W. Fluhr, A. Tfayli, R. Darlenski, M. E. Darvin, N. Joly-Tonetti, N. Lachmann, *J. Biophotonics* **2022**, e202200201. <https://doi.org/10.1002/jbio.202200201>